ELSEVIER

Materials Science and Engineering A353 (2003) 87–91

MATERIALS SCIENCE & ENGINEERING A

www.elsevier.com/locate/msea

APFIM investigations on site preferences, superdislocations, and antiphase boundaries in NiAl(Cr) with B2 superlattice structure

R. Fischer *, G. Frommeyer, A. Schneider

Max-Planck-Institut für Eisenforschung GmbH, Max-Planck-Str. 1, 40237 Düsseldorf, Germany

Abstract

The effect of the ternary element chromium in B2 ordered NiAl based alloys was studied by atom probe field ion microscopy. Samples of the compositions $Ni_{50}Al_{48}Cr_2$, $Ni_{49}Al_{49}Cr_2$, and $Ni_{48}Al_{50}Cr_2$ were investigated after different heat treatments. The chromium concentrations of the NiAl matrix, measured by atom probe, increased with increasing Ni/Al ratio and heat treatment temperature. The site preference of solute Cr atoms for the Al sublattice was determined by layer resolved measurements. An antiphase boundary observed in $Ni_{50}Al_{48}Cr_2$ showed a high local Cr concentration with Cr atoms substituting for Al atoms. Superdislocations in the quasi-stoichiometric $Ni_{49}Al_{49}Cr_2$ were not dissociated into partial dislocations and showed no Cr segregation. These results are discussed in view of activation of $a\langle 1\,1\,1\rangle$ slip systems.

Keywords: NiAl(Cr); Atom probe field ion microscopy; Antiphase boundary; Superdislocation

PACS numbers: 61.72.Ff; 61.72.Ss; 68.35.Dv; 68.37.Vj

1. Introduction

Due to its promising properties—low density, high melting point, thermal conductivity, and excellent oxidation resistance—the B2 ordered intermetallic NiAl compound has been investigated in view of high temperature applications for more than three decades [1,2]. However, a serious shortcoming is its low ductility below the brittle-to-ductile transition temperature. The von Mises criterion of five independent slip systems is not fulfilled for NiAl because only the $a\langle 0\,0\,1\rangle\{1\,1\,0\}$ slip system is active [3,4]. Slip in $a\langle 1\,1\,1\rangle$ direction is energetically unfavourable because an $a/2$ translation produces an antiphase boundary (APB) which is characterized by a high APB energy [4]. Linear muffin-tin orbital calculations predicted a considerable decrease in the APB energy by alloying with chromium in which the extent of the reduction depends on the substitutional behaviour [5]. Cr on Al sites was reported to lower the APB energy more significantly than Cr on Ni sites. Site preferences of Cr in B2 ordered NiAl have been calculated in [7,8] and experimentally measured in [9–11] using atom location by channeling enhanced microanalysis. Generally it was detected that Cr atoms preferentially occupy the Al sublattice. However, in [11] being the only experimental site preference study in which the Ni/Al ratio was varied a preference for the Ni sublattice in an Al-rich $Ni_{48}Al_{50}Cr_2$ alloy was observed.

An APB in NiAl(Cr), detected by APFIM, revealed strong Cr segregations [12] which showed good agreement with the results of the computer simulations in [5]. Dissociation of $a\langle 1\,1\,1\rangle$ superdislocations into $a/2\langle 1\,1\,1\rangle$ partial dislocations reduces energy of the moving dislocation and the lattice strain and produces an APB. The equilibrium state will be reached by the release of the lattice distortion energy and the formation energy of the built up APB. Therefore the dissociation width is a measure for estimating the ABP energy taking the elastic constants into account as described in [13].

2. Experimental procedure

Alloys of the nominal compositions: $Ni_{50}Al_{48}Cr_2$, $Ni_{49}Al_{49}Cr_2$, and $Ni_{48}Al_{50}Cr_2$ as well as pure NiAl

* Corresponding author. Tel.: +49-211-67-92-426; fax: +49-211-67-92-295.

E-mail address: fischer@mpie.de (R. Fischer).

0921-5093/02/$ - see front matter
PII: S0921-5093(02)00672-X

were produced by vacuum induction melting using high purity aluminium (99.99%), eletrolytic nickel (99.93%), and chromium (99.9%) with subsequent casting. The specimens were heat treated at 1200 °C for 100 h or at 550 °C for 500 h. All the samples were furnace cooled with a cooling rate of 50 K h^{-1}. The slow cooling rate was chosen in order to reduce the brittleness which can result in breaking of the material during cutting the samples or when applying high voltages in the field ion microscope. Water-quenched sample material showed a strong formation of cracks. Also quenching in of thermal vacancies should be avoided. Specimen blanks were cut by spark erosion. The sample tips were prepared by pre-electropolishing in a 5 vol.% solution of perchloric acid in acetic acid at 20–30 V d.c. and by final micropolishing in a 3 vol.% solution of perchloric acid in 2-butoxy-ethanol at 2–6 V d.c.

APFIM investigations were performed using the atom probe field ion microscope at the Max-Planck-Institut für Eisenforschung, Düsseldorf, described elsewhere [14]. The specimen temperature was 70–80 K. The basic pressure of the UHV chamber was about 2×10^{-10} mbar. Neon was used as imaging gas of a partial pressure of typically 5×10^{-5} up to 1×10^{-4} mbar. In atom probe experiments high pulse ratios of 25% were applied in order to prevent preferential evaporation of one of the atomic species. The pulse frequency was 200 Hz. Typically a detection rate of 0.003 ions per pulse was adjusted.

3. Results

3.1. Chromium contents and site preferences

The FIM imaging properties of NiAl and NiAl(Cr) and its behaviour in atom probe experiments have been described in greater detail in [15,16] and [12,17], respectively.

In FIM images the Cr-containing NiAl matrix shows a high degree of order as shown in Fig. 1 in which many high index poles can be recognized. In all of the investigated alloys and for both heat treatments Cr contents have been measured by atom probe surveys. Chromium precipitation in the investigated alloys has been described by the authors in [12]. The ⟨0 0 1⟩, ⟨1 1 1⟩, and ⟨1 1 3⟩ directions were chosen as measurement directions to avoid systematic errors by the choice of an unreliable measurement direction. No systematic connection between the measurement direction and the Cr content was detected. Ni, Al, and Cr desorbed as twofold charged ions, also a very small fraction of threefold charged Al^{3+} ions was often observed in the mass spectra due to the high pulse fraction. The measured Cr contents are shown in Fig. 2. Obviously the Cr content increases with increasing Ni content. In the Al-rich composition even after 1200 °C/100 h heat treatment the Cr content is very low. This behaviour would be in accordance with a site preference of the Cr atoms for the Al sublattice with only little influence of the Ni/Al ratio in the investigated composition range.

Site preferences in the materials heat treated at 1200 °C/100 h were investigated by layer resolved atom probe measurements along the ⟨0 0 1⟩ direction with atomic layer resolution. The results are shown in Table 1. About 70% of the detected Cr atoms in the three investigated alloys are occupying Al sites. Due to the anisotropic desorption behaviour a fraction of the Al ions is frequently not registered in atom probe surveys along the ⟨0 0 1⟩ direction. Therefore it is difficult to achieve atomic layer resolution and a correct determination of the composition at the same time. For this, the measurements frequently have to be interrupted in order to readjust the probe hole alignment. Residual Cr atoms are not appearing as bright spots in FIM images after desorption of either Al or Ni atom layers and thus their desorption field strength is not higher than those of Ni and Al atoms. A relatively large fraction of Cr atoms was detected close to the points in the ladder diagram mark the transition from Ni to Al layers. This occurs mostly at the first desorption processes of Al layers or at the final desorption of Ni layers. This is illustrated in the typical ladder diagram in Fig. 3. Considering the relatively low evaporation field of Cr atoms we assume that they desorb after the covering layer is removed and before they are in an edge-of-layer position. Therefore, Cr atoms which are desorbing when a Ni layer is collapsing emerge from an Al layer. Still a fraction of Cr were determined to emerge from Ni sites for certain so that a fraction of the Cr at the end of Ni layer in the ladder diagrams emerged from Ni sites as well. For this reason and especially as the layer resolution was not a perfect one large error bars given in Table 1 are present.

3.2. Antiphase boundaries and superdislocations

An APB was detected in $Ni_{50}Al_{48}Cr_2$ after thermal treatment at 550 °C/500 h by the authors which is described in [12,17]. A FIM image of the APB which possesses {1 2 3} plane orientation is shown in Fig. 4. The concentration profiles of the APB revealed a strong local Cr segregation in the APB with the Cr atoms occupying the Al sublattice (Fig. 5). It should be noted that the layer resolution is disturbed as long as parts of both antiphase domains lie under the probe hole. Therefore the site preference of the segregated Cr atoms in the APB plane can not be determined for certain while in the vicinity it is measurable.

The Gibbsian interfacial excess Γ_{Cr}^{APB} [18,19] was calculated to $\Gamma_{Cr}^{APB} = 46$ atoms nm^{-2} [17]. A grown-in APB was detected because the sample was not deformed

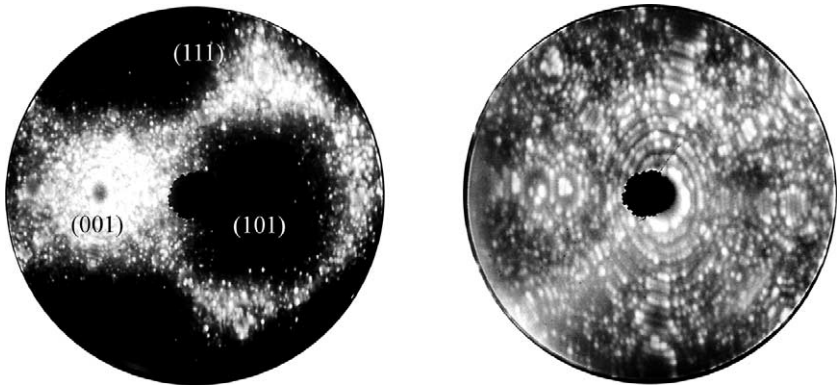

Fig. 1. (a) FIM image of the $Ni_{49}Al_{49}Cr_2$ matrix, heat treated 1200 °C/100 h. The strong differences in the brightness are caused by faceting of the tip surface. Image voltage: $U_{tip} = 16.0$ kV. (b) (0 0 1) pole after field desorption of about 50 Al+Ni double layers. The screen edge intersects the poles of {1 1 3} orientation. The high index poles reveals a high degree of ordering. $U_{tip} = 17.5$ kV.

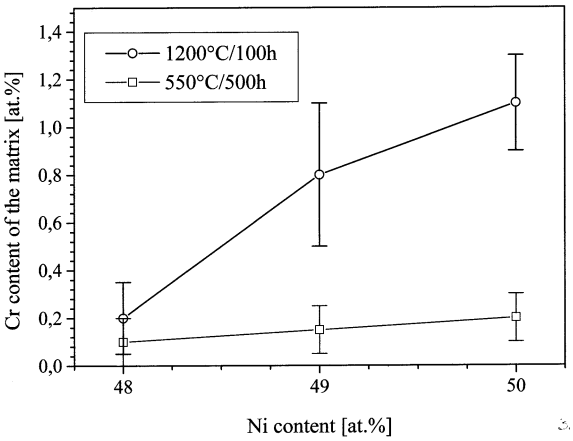

Fig. 2. Cr concentrations determined by APFIM measurements in the NiAl matrix depending on the composition and on the different heat treatment procedures of NiAl—2 at.% Cr measured by atom probe surveys.

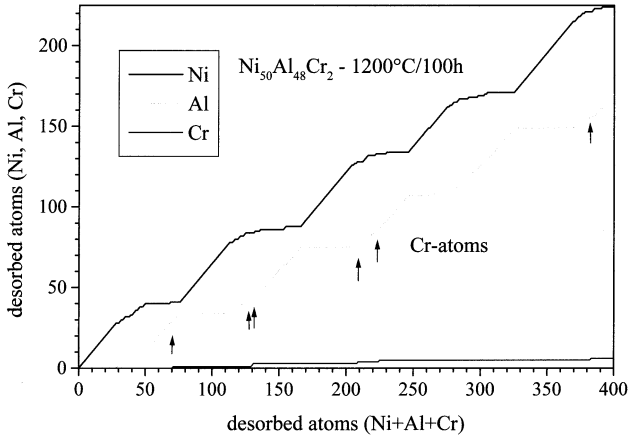

Fig. 3. Ladder diagram of the Cr–containing NiAl matrix in [0 0 1] direction. Cr atoms which are indicated by arrows are preferably located in Al layers.

Table 1
Site preferences of Cr atoms for the Al sublattice in B2 ordered Ni–Al—2 at.% Cr after heat treatment at 1200 °C per 100 h depending on composition measured by layer resolved atom probe surveys in ⟨0 0 1⟩ direction

Composition	Preference of Cr atoms for the Al sublattice (%)
$Ni_{48}Al_{50}Cr_2$	69 ± 14
$Ni_{49}Al_{49}Cr_2$	72 ± 7
$Ni_{50}Al_{48}Cr_2$	70 ± 10

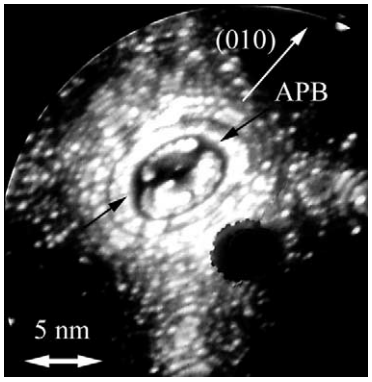

Fig. 4. FIM image of the {1 2 3} APB trace—indicated by arrows—crossing the (0 0 1) pole in $Ni_{50}Al_{48}Cr_2$. Heat treatment: 550 °C/500 h. $U_{tip} = 13.5$ kV.

and the produced thermal tension was kept relatively low. The terminating lines of the APB—grain boundaries or possibly dislocations—are located in an area that was etched away during sample preparation.

Superdislocations were observed in the quasi-stoichiometric composition $Ni_{49}Al_{49}Cr_2$ after 1200 °C/100 h heat treatment [17]. An example is shown in the desorption sequence in Fig. 6. In the FIM image the dislocation turns the (0 0 1) pole ring pattern into a double spiral in (a) and (b) and is shifted out of the (0 0 1) pole in [1 1 0] direction during desorption in (c). As the burgers vector possesses appreciable components in [0 0 1] and [1 1 0] direction we assume a $a\langle 1\,1\,1\rangle$ superdislocation. Neither dissociation of the superdislo-

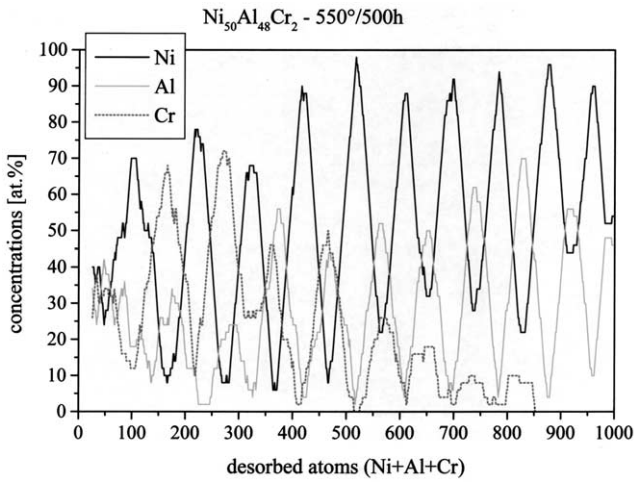

Fig. 5. Layer resolved Ni, Al, and Cr concentration profiles representing the APB in the first stages of appearance. The {1 2 3} APB shifts out of the probe hole during the atom probe measurement in [0 0 1] direction. Concentrations averaged over d$x = 50$ atoms. The nonstoichiometric composition at the end of the measurement shows an artefact caused by the probe hole alignment.

cation nor unusual high Cr concentration were detected in any of the dislocations.

4. Discussion

The Cr concentrations of about 1 at.% in the NiAl matrix determined by APFIM are in good agreement with the results of the investigation by Field et al. [9] and by Cotton et al. [10]. It has to be taken into consideration that these results were obtained after a cooling process of the samples in which precipitation occurred so that they are lower than the solubilities at the heat treatment temperature. The phase diagram data of Ni–Al–Cr in the literature as quoted in [20–22] give much higher Cr solubilities in the temperature range of 1000–1300 °C. These are based on electron probe microanalysis (EPMA) measurements. In contrast, TEM and APFIM show a much higher local resolution. Therefore small precipitates do not contribute to the measured Cr content.

The Cr contents of the NiAl matrix of NiAl—2 at.% Cr alloys with 48, 49, and 50 at.% Ni content detected in our investigations are comparable to those of the samples (NiAl—1 at.% Cr alloys with 50, 49.5, and 49 at.% Ni content) investigated using TEM by Cotton et al. [10] after heat treatment at 1400 °C/24 h where it was observed that the first two alloys were single-phase while the third was two-phase. This was interpreted by a Cr solubility of approximately 1 at.% for the quasi-stoichiometric composition with linearly increasing Cr content with increasing Ni content [10]. On the other hand the experimental results contradict the thermodynamic calculations of Huang and Chang [22] at $T =$ 1200 °C stating a shallow minimum of the Cr solubility at the quasi-stoichiometric composition because in this case solute Cr atoms would disturb the high degree of ordering. However, these calculations were adapted to the above mentioned phase diagram data—which do not show this minimum—and thus describe a relatively high Cr solubility. At the quasi-stoichiometric composition solute Cr atoms which preferentially occupy the Al sublattice should increase the number of vacancies in the Ni sublattice. While the quantification of vacancies was not possible by APFIM X-ray diffraction measurements showed a considerable decrease in the lattice constant a induced by alloying with Cr from $a = 0.28867 \pm 3 \times 10^{-5}$ nm for $Ni_{50}Al_{50}$ to $a = 0.28853 \pm 6 \times 10^{-5}$ nm for $Ni_{49}Al_{49}Cr_2$, both after heat treatment at 1200 °C/100 h (literature value: $0.28870 \pm 1 \times 10^{-5}$ nm [23] for pure NiAl). This decrease is produced by the additional vacancies and by the substitution of smaller Cr atoms for Al atoms. Furthermore this also means that alloying with Cr can result in an increased point defect density and consequently in point defect hardening.

In the three alloys we investigated approximately 70% of the solute Cr atoms are located on Al sites. Generally, the determined Al site preference is in good agreement with the literature data [6–10]. While the results for $Ni_{50}Al_{48}Cr_2$ and $Ni_{49}Al_{49}Cr_2$ are in accordance with

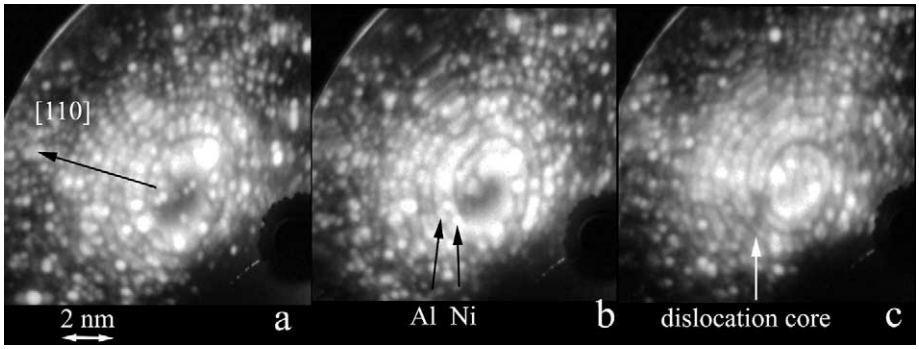

Fig. 6. FIM images of field desorption sequence of a superdislocation in $Ni_{49}Al_{49}Cr_2$ after revealing a double spiral in (a) and (b). The dislocation core was shifted away from the topmost plane parallel to the [1 1 0] direction. Note that the dislocation core is below the centre of the topmost plane in (a) and (b). No dissociation of the superdislocation was indicated. The sample material was heat treated at 1200 °C/100 h; $U_{tip} = 20.0$ kV.

those of Tian et al. who investigated the same compositions a discrepancy occurred for the Al-rich alloy $Ni_{48}Al_{50}Cr_2$ [11]. Here only 34.2% of the Cr atoms were detected to occupy Al lattice sites. In this study a heat treatment different from ours was carried out: solution annealing at 1290 °C/1 h and subsequent quenching in iced water. However, in [11] the amount of solute Cr in the corresponding alloy is not indicated and measurement errors resulting from precipitation are not discussed. In comparison to our results it is not clear whether (1) the Cr content in the NiAl phase of the Al-rich alloy was significantly lower than 2 at.% after the 1290 °C heat treatment and quenching and consequently precipitation of Cr lead to an error in the site preference determination—this was pointed out by Cotton et al. in [10]—or (2) the 2 at.% Cr could be dissolved and precipitation could be suppressed so that the site preference in fact showed a strong dependence on the thermal treatment. For the Ni-rich and the quasi-stoichiometric compositions complete solution or a much less significant error by precipitation appears to be much more probable.

Calculations of {1 1 0} APB energies in pure and Cr-containing NiAl by Hong and Freeman lead to the conclusion the that the APB energy is lowered by Cr addition and that this effect is strongest when Cr atoms substitute for Al atoms [5]. Although the APB described in this work possesses a different orientation the observed high local Cr concentration and the substitutional behaviour of the Cr atoms are strikingly similar to the model situation with the lowest APB energy. However, the Cr content in NiAl is low (≈ 1 at.%), and APBs are rare in NiAl(Cr). Therefore the formation of APBs in the NiAl(Cr) matrix should still be energetically unfavourable. Accordingly superdislocations are more favourable compared to partial dislocations and the dissociation of superdislocations is suppressed as directly observed by FIM in our investigations [17]. The TEM studies of Field et al. [9] revealed undissociated $a\langle 1\,1\,1\rangle$ dissociations. Also calculations by Fu and Yoo [4] state that the dissociation of $a\langle 1\,1\,1\rangle$ dissociations in NiAl is improbable. Corresponding to the high ABP energy it is also reported that $\langle 1\,1\,1\rangle$ slip is not significantly activated in Cr alloyed NiAl [3].

Acknowledgements

The financial support by the Deutsche Forschungsgemeinschaft, DFG, Schwerpunktprogramm 'Strukturgradienten in Kristallen', is gratefully acknowledged.

References

[1] D.B. Miracle, Acta Metall. Mater. 41 (1993) 649.
[2] D.B. Miracle, R. Darolia, in: J.H. Westbrook, R.L. Fleischer (Eds.), Intermetallic Compounds, vol. 2, Wiley, 1994, p. 53.
[3] J.D. Cotton, R.D. Noebe, M.J. Kaufmann, Intermetallics 1 (1993) 117.
[4] C.L. Fu, M.H. Yoo, Acta Metall. Mater. 40 (1992) 703.
[5] T. Hong, A.J. Freeman, Phys. Rev. B 43 (8) (1991) 6446.
[6] N.I. Medvedeva, Y.N. Gornostyrev, D.L. Novikov, O.N. Mryasov, A.J. Freeman, Acta Mater. 46 (1998) 3433.
[7] G. Bozzolo, R.D. Noebe, J. Ferrante, A. Garg, Mater. Sci. Eng. A 239 (1997) 769.
[8] G. Bozzolo, R.D. Noebe, F. Honecy, Intermetallics 8 (2000) 7.
[9] R.D. Field, D.F. Lahrmann, R. Darolia, Acta Metall. Mater. 39 (12) (1991) 2961.
[10] J.D. Cotton, R.D. Noebe, M.J. Kaufmann, Intermetallics 1 (1993) 3.
[11] W.H. Tian, C.S. Han, M. Nemoto, Intermetallics 7 (1999) 59.
[12] R. Fischer, G. Frommeyer, A. Schneider, Mater. Sci. Eng. A., 271 (2002) 47.
[13] P. Veyssière, R. Noebe, Phil. Mag. 65 (1992) 1.
[14] H.-J. Habrock, Ph. D. Thesis, Technische Universität Clausthal (1989).
[15] Z.G. Liu, G. Frommeyer, M. Kreuß, Surf. Sci. 246 (1991) 272.
[16] M.K. Miller, R. Jayaram, Surf. Sci. 266 (1992) 458.
[17] R. Fischer, G. Frommeyer, A. Schneider, Phys. Stat. Sol. (a) 186 (2001) 115.
[18] M.K. Miller, A. Cerezo, M.G. Hetherington, G.D.W. Smith, Atom Probe Field Ion Microscopy, Clarendon Press, Oxford, 1996.
[19] B.W. Krakauer, D.N. Seidman, Acta Mater. 46 (1998) 6145.
[20] S.M. Merchant, M.R. Notis, Mat. Sci. Eng. 66 (1984) 47.
[21] P. Rogl, in: G. Effenberg, G. Petzow (Eds.), Ternary Alloys, VCH, Weinheim, 1991, p. 400.
[22] W. Huang, Y.A. Chang, Intermetallics 7 (1999) 863.
[23] A. Taylor, N.J. Doyle, J. Appl. Cryst. 5 (1972) 201.